

## Conformational Analysis of A $\beta$ -(25–35) Peptide by NMR: Insights into Secondary Structure and Aggregation Propensity

Gulyaz Najafova Zulfu <sup>1,\*</sup>, Gulshen Agaeva Alakbar <sup>2</sup>, Kelton Rodrigues de Souza <sup>3</sup> and Philippe Bertani <sup>4</sup>

<sup>1</sup> French-Azerbaijani University – (UFAZ) under Azerbaijan State Oil and Industry University, 183 Nizami St, Baku, Azerbaijan

<sup>2</sup> Institute for Physical Problems, Baku State University, AZ-1148, Baku, Z.Khalilov Str.23, Azerbaijan

<sup>3</sup> Laboratoire de RMN et biophysique des membranes, UMR 7177, Institut de Chimie de Strasbourg, Université de Strasbourg CNRS, 4Rue Blaise Pascal 67081, Strasbourg, France

**Abstract:** In Alzheimer's disease, amyloid  $\beta$  (A $\beta$ ) is a principal component that accumulates within neuritic plaques. This disease is characterized by the aggregation of the protein A $\beta$  (amyloid  $\beta$ ) in the brain. Sequence GSNKGAIIGLM (A $\beta$  25–35) is the shortest toxic fragment of the protein A $\beta$ -peptide, able to reproduce the aggregation process. NMR spectroscopy was utilized to investigate the spatial arrangement of the  $\beta$ -amyloid (25–35) peptide, which had been solubilized in water and HFIP at 25°C and prepared with an 80:20 D<sub>2</sub>O/H<sub>2</sub>O solvent mixture (900  $\mu$ L). The XPLOR-NIH software (version 2.27) was used for the calculation and refinement of the three-dimensional structures. Using MOLMOL, the lowest-energy ten structural models were depicted and evaluated. NMR analysis of the A $\beta$ -(25–35) peptide dissolved in the 20/80 HFIP and water mixture revealed that the C-terminal area tends to form more organized conformations, in contrast to the predominantly disordered nature of the N-terminal region observed in the structural overlays. Such conformational properties are anticipated to facilitate the design of molecules that can associate with amyloid peptides and act as inhibitors of their aggregation into fibrils.

**Keywords:** Amyloid  $\beta$  -(25-35) peptide, NMR spectroscopy, conformation, secondary structure.

### 1. Introduction

Alzheimer's disease (AD) is one of the most common neurodegenerative disorders, characterized by progressive memory loss and cognitive decline <sup>1,2</sup>. A pathological characteristic of AD is the formation of amyloid plaques in the brain, which are primarily composed of aggregated amyloid  $\beta$  protein (A $\beta$ ) <sup>1,3,4</sup>. Research has shown that proteins and peptides can transform from their native functional states into amyloid assemblies <sup>5</sup>. Such aggregates, referred to as amyloids, are built from misfolded peptides or proteins aligned in a cross- $\beta$  arrangement, a property that contributes to their increased resistance to proteolytic enzymes <sup>1–3</sup>. The buildup of these protein aggregates in diverse tissues of animals and humans is connected to the progression of various pathological conditions, among them Alzheimer's disease.

The amyloid  $\beta$  protein (A $\beta$ ) plays a key role in AD; its misfolding and aggregation lead to the formation of neurotoxic oligomers and insoluble amyloid fibrils that form the plaques. Understanding the conformational changes of A $\beta$  is crucial for

elucidating the molecular basis of AD and for developing therapeutic strategies <sup>6</sup>. Although A $\beta$  aggregation plays a central role in AD pathogenesis, the molecular mechanisms driving amyloid formation in vivo remain incompletely understood. Thus, in vitro models of amyloid formation are valuable tools for studying the aggregation process, as the ability to form amyloid-like structures is a universal property of polypeptide chains <sup>7–9</sup>. These models allow for controlled investigation of factors influencing A $\beta$  aggregation. Several proteins have been identified to form amyloid-like aggregates or fibrils under specific in vitro conditions <sup>10,11</sup>.

Among the various fragments of the A $\beta$  peptide, the sequence GSNKGAIIGLM, known as A $\beta$  (25–35), is particularly significant. It represents the shortest toxic fragment of the A $\beta$  peptide and is capable of reproducing the aggregation process observed in the full-length protein <sup>12</sup>. Figure 1 highlights the A $\beta$  (25–35) peptide fragment in the full A $\beta$ 42 protein sequence (DAEFRHDSGYEVHHQKLVFFAEDVGSNKGAIIGLMVGGVVIA).

\*Corresponding author: Gulyaz Najafova

Email address: [gulyaz.najafova@ufaz.az](mailto:gulyaz.najafova@ufaz.az)

DOI: <http://dx.doi.org/10.13171/mjc02508211853najafova>

Received April 21, 2025

Accepted April 7, 2025

Published August 21, 2025

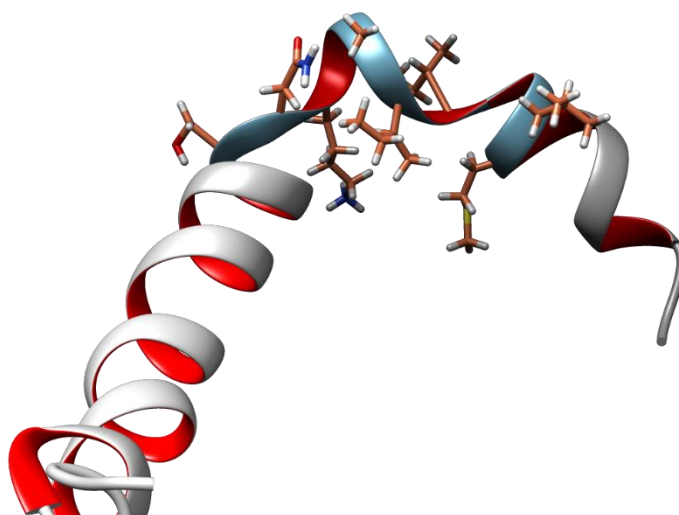


**Figure 1.** Structure of A $\beta$  monomer protein (A $\beta$ 42). The structure highlights the position of the A $\beta$  (25–35) fragment (sky blue color in the external part, ribbon helix interior in red color) within the full-length A $\beta$  sequence. PDB 1IYT.

Previous studies have investigated the conformational behavior of A $\beta$  (25–35) and its fragments under different conditions, suggesting that their secondary structure content is highly dependent on solution conditions<sup>13,14</sup>. For instance, NMR experiments performed on A $\beta$  (25–35) in a 50% aqueous solution of 2,2,2-trifluoroethanol (TFE) revealed that the peptide adopts an  $\alpha$ -helical conformation and does not aggregate in the presence of TFE<sup>15</sup>. Other studies have further investigated the A $\beta$  (25–35) peptide<sup>16–18</sup> using NMR spectroscopy in different TFE/water solutions, showing distinct conformational behaviors. As reported, TFE is known to act as a secondary structure-inducing agent<sup>18</sup>.

Nuclear Magnetic Resonance (NMR) spectroscopy is a powerful technique for determining the spatial and secondary structures of peptides and proteins in solution, providing atomic-level insights into their conformational dynamics. Studies using such powerful spectroscopies are vital for understanding how environmental factors influence peptide folding and aggregation. Given the critical role of secondary structure in amyloid formation, NMR can provide key insights into the structural transitions of A $\beta$  peptides. In addition, understanding the conformational structure of the A $\beta$  peptide, particularly fragments like A $\beta$  (25–35), may provide important insights into the pathogenesis of Alzheimer's disease. By characterizing the structural features that promote or inhibit aggregation, the researchers can identify potential targets for therapeutic intervention.

Similar to TFE, 1,1,1,3,3,3-Hexafluoro-propan-2-ol (HFIP) is one of the most common and effective cosolvents for the structural stabilization of peptides that form secondary structures<sup>19</sup>. HFIP is a polar organic compound with strong hydrogen bond-donating properties widely used in organic synthesis. However, since the influence of hexafluoroisopropanol (HFIP) on peptide

conformation is not well understood, we investigated the secondary structure of the A $\beta$  (25–35) fragment in a water/HFIP solution using NMR spectroscopy. Understanding the effects of solvents like HFIP is vital for gaining insights into protein folding, and consequently, for designing molecules capable of interacting with amyloid peptides as inhibitors of fibril formation, and thus contributing to the development of new strategies to combat Alzheimer's disease.

## 2. Materials and methods

TOCSY, NOESY, and HSQC experiments were performed on a Bruker Avance III HD 500 MHz spectrometer equipped with a Cryo-Sonde probe (Helium X-1H, 5 mm, 31P < X < 15N). The data were analyzed using CCPNMR and visualized with JRAMA+ software. The assignments were then submitted to TALOS+ online for chemical shift analysis.

### 2.2. Peptide sample preparation

The A $\beta$  (25–35) peptide (GSNKGAIIGLM) was purchased from GeneCust peptides synthesis. We used a commercially available HCl salt form of the A $\beta$  (25–35) peptide (without TFA). The purity of the peptide was estimated to be higher than 95% according to mass spectrometry and HPLC control data provided by GeneCust.

The solubilization procedure for the A $\beta$  (25–35) peptide was adapted from<sup>20</sup>. For solution NMR, we first prepared a 10 mM peptide solution by dissolving 10.6 mg of the peptide in 1 mL of HFIP (Sigma Aldrich, France). Then, we mixed 100  $\mu$ L of the 10 mM peptide solution with 900  $\mu$ L of D<sub>2</sub>O/H<sub>2</sub>O (80/20) (deuterium oxide in water) to achieve a final peptide concentration of 1 mM in a 1 mL solution. (*Regions of collagen triple helix structure*)

## 2.2. NMR solution structure calculation

Two-dimensional NMR solution experiments (NOESY, TOCSY, and  $^1\text{H}$ - $^{13}\text{C}$  HSQC) were recorded on a Bruker Avance spectrometer (Bruker, Germany) operating at a frequency of 500.13 MHz for protons. The experiments were carried out to determine the three-dimensional structure of the A $\beta$  (25–35) peptide. The samples consisted of an aqueous solution of 1 mM A $\beta$  (25–35), containing 10% (v/v) D $_2$ O/H $_2$ O and 1% (v/v) 2,2-dimethyl-2-silapentane-5-sulfonate- $d_6$  (DSS- $d_6$ ) as the internal reference. A 4 mm triple resonance NMR cryoprobe was used for all experiments. Water suppression was achieved using a WATERGATE pulse sequence <sup>21</sup>.

Two-dimensional homonuclear Total Correlation Spectroscopy (TOCSY) spectra were acquired using a pulse sequence with a mixing time of 80 ms, 576  $t_1$  increments, and 32 transients of 6008 points for a spectral width of 6009.6 Hz <sup>22</sup>. Nuclear Overhauser Effect Spectroscopy (NOESY) spectra were obtained using mixing times of 120, 150, and 200 ms to check for spin diffusion, with 576  $t_1$  increments and 32 transients of 6008 points for a spectral width of 6009.1 Hz <sup>22</sup>.

Heteronuclear Single Quantum Coherence ( $^1\text{H}$ - $^{13}\text{C}$  HSQC) experiments were performed in edited mode,

where CH $_2$  correlations appear with a negative phase, and CH and CH $_3$  correlations appear with a positive phase <sup>23</sup>. The data were recorded with F1 and F2 spectral widths of 22,640.47 Hz and 7042.25 Hz, respectively. A total of 640  $t_1$  increments were accumulated with 16 transients of 3520 points.

Proton resonances were assigned through simultaneous analysis of homonuclear  $^1\text{H}$ ,  $^1\text{H}$ -TOCSY, and  $^1\text{H}$ ,  $^1\text{H}$ -NOESY spectra using the Wüthrich method <sup>24</sup>. Heteronuclear spectra were used as additional confirmation. The NMR assignments were performed manually using the NMRViewJ software (version 9.2.0-b20) <sup>25</sup>. NOE intensities were converted into semi-quantitative distance restraints with upper limits of 2.8, 3.4, and 5.0 Å <sup>26</sup>. Dihedral angle restraints were obtained from the chemical shifts of HN, H $\alpha$ , H $\beta$ , C $\alpha$ , C $\beta$ , and N using the TALOS+ program <sup>27</sup> within the NMRPipe® computational package <sup>28</sup> (Table 1). The  $^{13}\text{C}\alpha$  chemical shift index was calculated according to the Wishart method <sup>29</sup>. Geometric restraints were validated for consistency and contribution using the QUEEN program (Quantitative Evaluation of Experimental NMR Restraints) <sup>30</sup>.

**Table 1.** In red, we can see the dihedral angles of the ab peptide. This result can be seen in JRAMA+ viewer and in the phi, psi-dihedral angles – abpeptide.txt file.

VARS	RESID	RESNAME	PHI	PSI	DPHI	DPSI	DIST	S2	COUNT	CS_COUNT	CLASS
FORMAT	%4d	%s	%8.3f	%8.3f	%8.3f	%8.3f	%8.3f	%5.3f	%2d	%2d	%s
2	S	-0.000	-0.000	0.000	0.000	0.000	0.000	0	9	None	
3	N	-68.092	-40.687	13.545	16.455	48.768	0.699	10	13	Good	
4	K	-62.940	-32.888	5.122	12.208	46.505	0.707	10	12	Good	
5	G	-65.520	-38.722	10.005	14.563	47.039	0.732	10	12	Good	
6	A	-63.676	-41.176	5.685	6.146	46.265	0.752	10	13	Good	
7	I	-63.029	-43.836	9.191	4.562	35.617	0.794	10	14	Good	
8	I	-62.727	-43.605	8.705	4.120	40.315	0.807	10	14	Good	
9	G	-61.344	-37.580	7.294	24.158	44.763	0.791	10	14	Good	
10	L	-71.214	-35.302	11.589	13.207	78.754	0.728	10	13	Good	
11	M	9999.00	9999.00	0.00	0.00	0.00	0.00	0	9	None	

The XPLOR-NIH software (version 2.27) was used for the calculation and refinement of the three-dimensional structures <sup>31,32</sup>. A total of 100 structures, starting from an extended conformation, were generated using a simulated annealing protocol in torsional angle dynamics. This included 20,000 steps of simulated annealing at 1000 K, followed by a temperature decrease over 15,000 steps in the initial

slow-cooling stage. The resulting structures were then refined in a subsequent calculation using more stringent topology parameters (ref\_sa\_new.php) <sup>33</sup>. The ten lowest-energy structures were visualized and analyzed using MOLMOL<sup>20</sup> and Chimera <sup>34</sup>. Structural quality was assessed using Ramachandran plots and root-mean-square deviation (RMSD) values, both obtained via the PSVS online platform <sup>35</sup> (Figure 2).

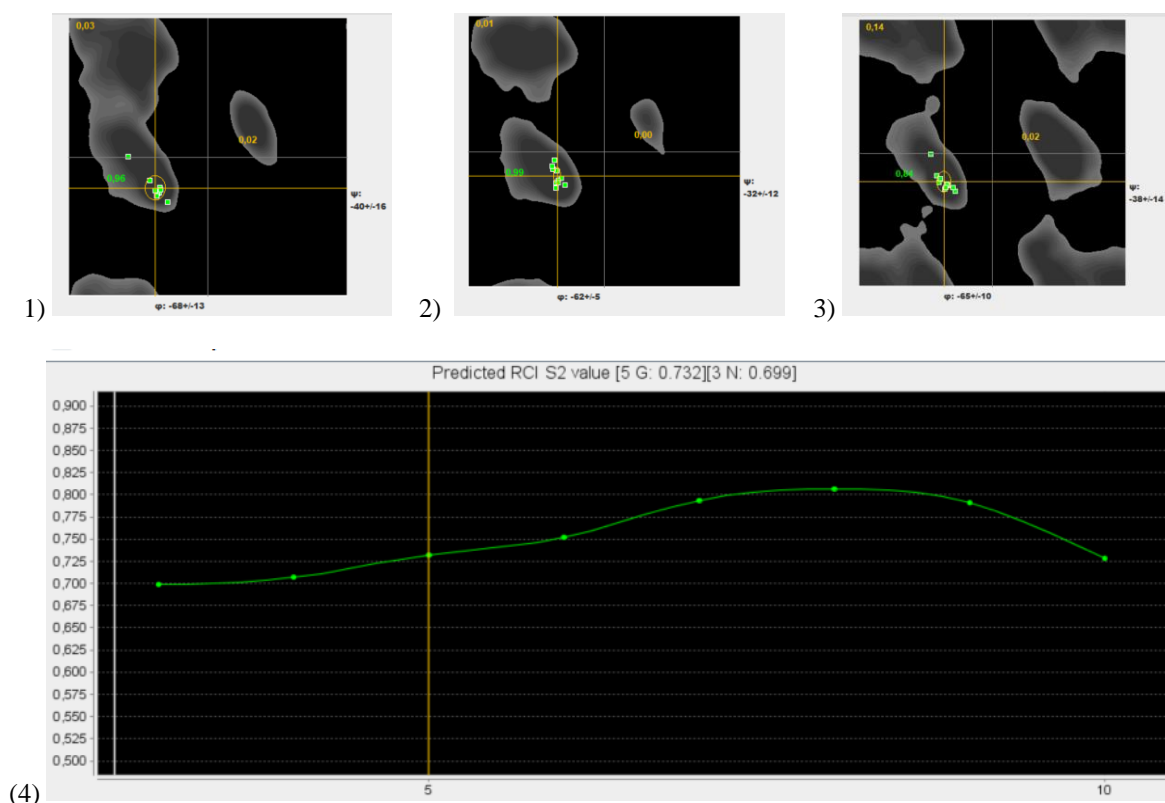


**Figure 2.** 1) Dihedral angles of residue N3, 2) K4, and 3) G5. 4) Predict RCI – Secondary structures and Motifs.

### 3. Results and Discussion

Several studies have established a correlation between soluble A $\beta$  and Alzheimer's disease, with evidence suggesting that soluble A $\beta$  peptides play an essential role in the pathogenesis and advancement of this disease <sup>36</sup>. Therefore, elucidating the soluble monomeric conformation of the A $\beta$  (25–35) peptide is of great importance, as this conformation may profoundly influence the nature of early aggregates and the resulting morphology of the amyloid fibril <sup>37</sup>.

To perform multidimensional solution NMR experiments, the A $\beta$  (25–35) peptide was solubilized in a water/HFIP solution at 25 °C. The sequential  $d_{\alpha N}$  ( $i, i+1$ ) connectivities are summarized in Figure 3.

Complete H, C, and N signals were assigned using a

combination of TOCSY, NOESY, and HSQC NMR experiments. The spin systems of the significant amino acid residues and their respective  $^1\text{H}$  and  $^{13}\text{C}$  chemical shifts were identified by analyzing intra-residual correlations in the TOCSY spectrum and the  $^1\text{H}$ – $^{13}\text{C}$  HSQC spectrum. The number of inter-residual cross-peaks detected in the NOESY contour map helped resolve all ambiguities. The NMR data suggest the absence of stable secondary structures, as no medium-range  $d_{\alpha N}$  ( $i, i+n$ ) contacts (with  $n = 2, 3$ , or 4) were detected in the NOESY spectra. These chemical shifts were then used for secondary structure and dihedral angle prediction using TALOS+, in which the chemical shift dispersion of alpha and amide protons indicates an unfolded peptide conformation (Figure 4).

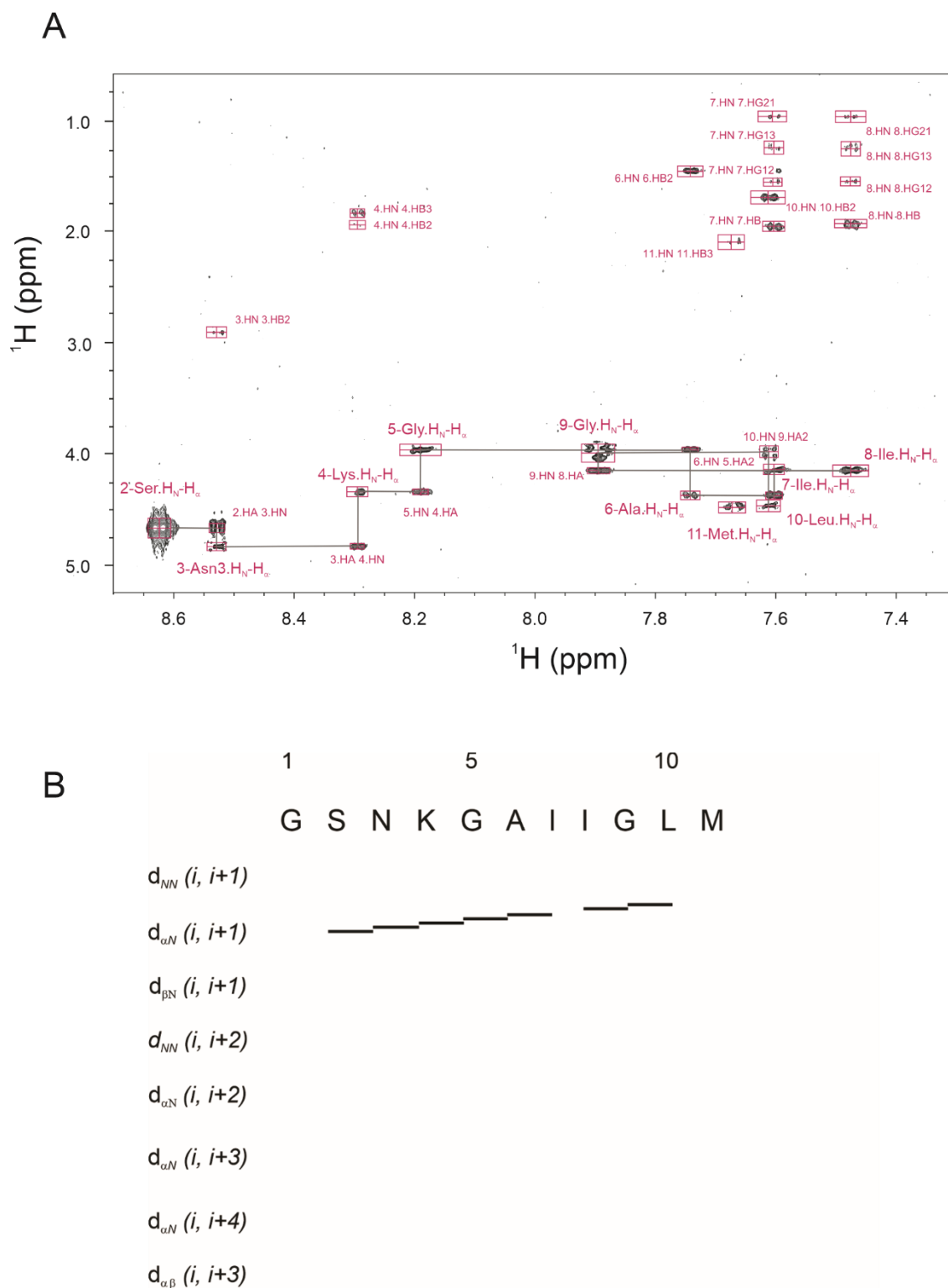


**Figure 3.** HN-H $\alpha$  region of NOESY spectrum of A $\beta$  (25-35) peptide at 1 mM in water/HFIP/D $_2$ O (A). Spectrum recorded at 25 °C, 500 MHz. Only the inter-residual HN-H $\alpha$  (i, i + 1) cross peaks are labeled.



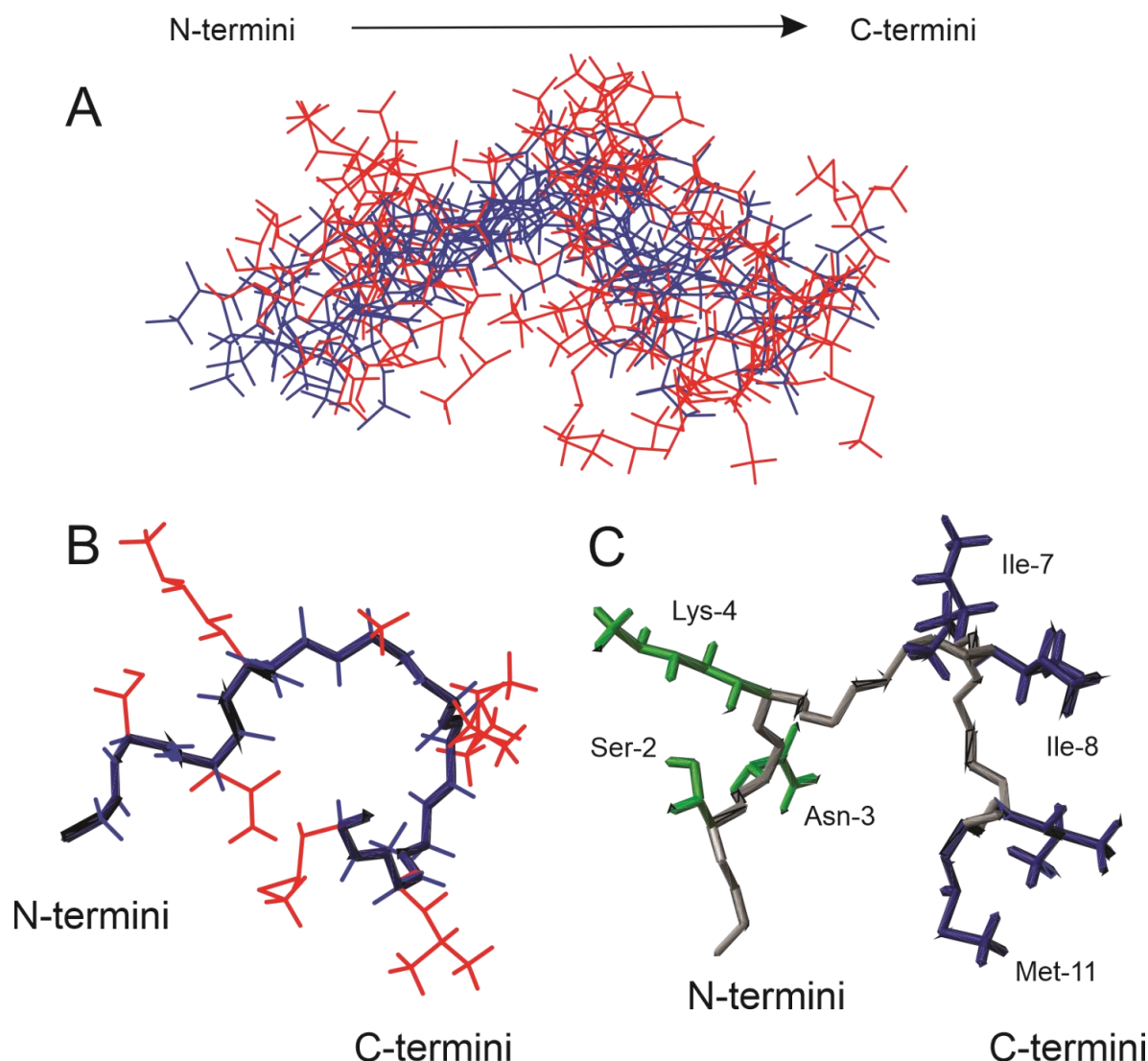


**Figure 4.** Three-dimensional structures of Aβ (25-35) peptide (1 mM) at 25°C obtained from NMR at 500 MHz. The superposition of the ten lowest-energy structures for ecPis-4s (from G1 to M11) (panel A). Horizontal perspective of the lowest-energy structure (panels B and C). The hydrophobic residues are presented in blue and the hydrophilic residues in green.

The superposition of the ten lowest-energy structures of the Aβ (25–35) peptide is shown in Figure 4, illustrating both backbone and side-chain orientations. The lowest-energy structure is also presented from two different perspectives. As observed, under the conditions of this study (water/HFIP solution), the Aβ (25–35) peptide secondary structure can be described ambiguously.

Overall, our spectroscopic data confirm that the conformational behavior of Aβ (25–35) is strongly environment-dependent. These conclusions have also been reached in many recent structural studies of Aβ (25–35) peptide<sup>38–42</sup>. Previous studies on Aβ peptide fibrillogenesis associated with familial cerebral amyloid angiopathy support this mechanism<sup>43</sup>. These studies showed that the model peptide can form both

unstructured and helix-turn-helix conformations<sup>44,45</sup>.

#### 4. Conclusions

The NMR-derived structures of the Aβ (25–35) peptide in a 20/80 HFIP and water mixture indicate that ordered arrangements are concentrated mainly in the C-terminal portion. The mean global backbone RMSD of the Aβ (25–35) peptide is  $3.39 \pm 0.96$  Å. When aligned based on the N-terminal segment (residues 1 to 5), the structures are well-fitted, with a global RMSD of  $1.49 \pm 0.35$  Å. The backbone region spanning residues 25 to 29 exhibited an RMSD of 1.49 Å. Understanding these conformational properties can contribute to creating molecules that target amyloid peptides and block fibril development.

## Conflict of interest

The authors declare that they have no conflicts of interest.

## References

1. Z. Breijyeh, R. Karaman, Comprehensive review on Alzheimer's disease: causes and treatment, *Molecules*, **2020**, 25(24), 5789.
2. I. Anjum, M. Fayyaz, A. Wajid, W. Sohail, Alzheimer disease, in StatPearls, StatPearls Publishing, Treasure Island (FL), **2023**.
3. J. Hardy, D.J. Selkoe, The amyloid hypothesis of Alzheimer's disease: progress and problems on the road to therapeutics, *Science*, **2002**, 297, 353–356.
4. D.J. Selkoe, J. Hardy, Alzheimer's disease: the amyloid hypothesis at 25 years, *EMBO Mol. Med.*, **2016**, 8, 595–608.
5. F. Chiti, C.M. Dobson, Protein misfolding, amyloid formation, and human disease: a summary of progress over the last decade, *Annu. Rev. Biochem.*, **2017**, 86, 27–68.
6. P.J. Crouch, D.J. Tew, T. Du, et al., Restored degradation of the Alzheimer's amyloid- $\beta$  peptide by targeting amyloid formation, *J. Neurochem.*, **2009**, 108, 1198–1207.
7. D.M. Fowler, A.V. Koulov, C. Alory-Jost, et al., Functional amyloid formation within mammalian tissue, *PLoS Biol.*, **2006**, 4, e6.
8. M. Stefani, C.M. Dobson, Protein aggregation and aggregate toxicity: new insights into protein folding, misfolding diseases and biological evolution, *J. Mol. Med. (Berl.)*, **2003**, 81, 678–699.
9. C.M. Dobson, Principles of protein folding, misfolding and aggregation, *Semin. Cell Dev. Biol.*, **2004**, 5, 3–16.
10. S.M. Dorta-Estremera, J. Li, W. Cao, Rapid generation of amyloid from native proteins in vitro, *J. Vis. Exp.*, **2013**, 82, 50869.
11. L. Goldschmidt, P.K. Teng, R. Riek, et al., Identifying the amyloids, proteins capable of forming amyloid-like fibrils, *Proc. Natl. Acad. Sci. U.S.A.*, **2010**, 107, 3487–3492.
12. O. Crescenzi, S. Tomaselli, R. Guerrini, et al., Solution structure of the Alzheimer amyloid  $\beta$ -peptide (1–42) in an apolar microenvironment, *FEBS J.*, **2002**, 269, 5642–5648.
13. K. Halverson, P.E. Fraser, D.A. Kirschner, P.T. Lansbury Jr., Molecular determinants of amyloid deposition in Alzheimer's disease, *Biochemistry*, **1990**, 29, 2639–2645.
14. C. Soto, E.M. Castaño, B. Frangione, N.C. Inestrosa,  $\alpha$ -Helical to  $\beta$ -Strand transition in the N-terminal fragment of A $\beta$  modulates amyloid formation, *J. Biol. Chem.*, **1995**, 270, 3063–3067.
15. S. Lee, Y.-H. Suh, S. Kim, Y. Kim, Comparison of  $\beta$ -amyloid (25–35) and substance P structures in TFE/water, *J. Biomol. Struct. Dyn.*, **1999**, 17, 381–389.
16. A. Sepehri, T. Lazaridis, Putative structures of membrane-embedded A $\beta$ -oligomers, *ACS Chem. Neurosci.*, **2023**, 14, 99–110.
17. A.B. Clippingdale, J.D. Wade, C.J. Barrow, The amyloid- $\beta$  peptide and its role in Alzheimer's disease, *J. Pept. Sci.*, **2001**, 7, 227–249.
18. S. Ohnishi, K. Takano, Amyloid fibrils from the viewpoint of protein folding, *Cell. Mol. Life Sci.*, **2004**, 61, 511–524.
19. N. Hirota, K. Mizuno, Y. Goto, Cooperative  $\alpha$ -helix formation of  $\beta$ -lactoglobulin and melittin induced by hexafluoroisopropanol, *Protein Sci.*, **1997**, 6, 416–421.
20. R. Koradi, M. Billeter, K. Wüthrich, MOLMOL: analysis of macromolecular structures, *J. Mol. Graph.*, **1996**, 14, 51–55.
21. M. Liu, X.A. Mao, C. Ye, et al., Improved WATERGATE for solvent suppression, *J. Magn. Reson.*, **1998**, 132, 125–129.
22. T.L. Hwang, A.J. Shaka, Water suppression by excitation sculpting, *J. Magn. Reson. A*, **1995**, 112, 275–279.
23. W. Willker, D. Leibfritz, R. Kerssebaum, W. Bermel, Gradient selection in inverse correlation spectroscopy, *Magn. Reson. Chem.*, **1993**, 31, 287–292.
24. K. Wüthrich, NMR with proteins and nucleic acids, *Europhys. News*, **1986**, 17, 11–13.
25. B.A. Johnson, R.A. Blevins, NMR View: visualization and analysis of NMR data, *J. Biomol. NMR*, **1994**, 4, 603–614.
26. S.G. Hyberts, M.S. Goldberg, T.F. Havel, G. Wagner, Eglin C solution structure and X-ray comparison, *Protein Sci.*, **1992**, 1, 736–751.
27. Y. Shen, F. Delaglio, G. Cornilescu, A. Bax, TALOS+: predicting torsion angles from NMR shifts, *J. Biomol. NMR*, **2009**, 44, 213–223.
28. F. Delaglio, S. Grzesiek, G.W. Vuister, et al., NMRPipe: a UNIX-based spectral processing system, *J. Biomol. NMR*, **1995**, 6, 277–293.
29. D.S. Wishart, B.D. Sykes, Chemical shifts in structure determination, *Methods Enzymol.*, **1994**, 239, 363–392.
30. S.B. Nabuurs, C.A.E.M. Spronk, G. Vriend, G.W. Vuister, Tools for NMR restraint validation, *Concepts Magn. Reson. A*, **2004**, 22, 90–105.
31. L.M. Rice, A.T. Brünger, Torsion angle dynamics for structure refinement, *Proteins*, **1994**, 19, 277–290.
32. E.G. Stein, L.M. Rice, A.T. Brünger, Torsion-angle dynamics in NMR calculations, *J. Magn. Reson.*, **1997**, 124, 154–164.
33. C. Schwieters, J. Kuszewski, G.M. Clore, Using Xplor-NIH for NMR structures, *Prog. Nucl. Magn. Reson. Spectrosc.*, **2006**, 48, 47–62.
34. E.F. Pettersen, T.D. Goddard, C.C. Huang, et al., UCSF Chimera: visualization system for research, *J. Comput. Chem.*, **2004**, 25,

- 1605–1612.
35. A. Bhattacharya, R. Tejero, G.T. Montelione, Evaluating structures from structural genomics consortia, *Proteins*, **2007**, 66, 778–795.
36. R. Sarroukh, E. Goormaghtigh, J.M. Ruyschaert, V. Raussens, ATR-FTIR: a "rejuvenated" tool to investigate amyloid proteins, *Biochim. Biophys. Acta*, 2013, **1828**, 2328–2338.
37. M.S. Celej, R. Sarroukh, E. Goormaghtigh, et al., Toxic prefibrillar alpha-synuclein amyloid oligomers adopt a distinctive antiparallel beta-sheet structure, *Biochem. J.*, **2012**, 443, 719–726.
38. G.A. Agaeva, G.Z. Najafova, A.D. Mammadova, Circular dichroism spectroscopy study of the spatial structure of  $\beta$ -amyloid peptide (25–35) in a medium with conditions similar to the membrane environment, *J. Appl. Spectrosc.*, **2025**, 92, 293–297.
39. Y. Fezoui, D.M. Hartley, D.M. Walsh, et al., A de novo designed helix-turn-helix peptide forms nontoxic amyloid fibrils, *Nat. Struct. Biol.*, **2000**, 7, 1095–1099.
40. S.A. Kurakin, O.I. Ivankov, T.N. Murugova, et al., Lipid membrane destabilization induced by amyloid-beta peptide in the systems mimicking preclinical Alzheimer's disease, *Nat. Sci. Rev.*, **2025**, 2, 100202.
41. A. Santoro, A. Ricci, M. Rodriguez, et al., A structural effect of the antioxidant curcuminoids on the A $\beta$  (1–42) amyloid peptide, *Antioxidants*, **2025**, 14, 53.
42. G.Z. Najafova, G.A. Agaeva, Z. Boubegtiten-Fezoua, A.F. Santos Seica, P. Hellwig, Conformational particularities of A $\beta$  (25–35) peptide determined by infrared spectroscopy, *Adv. Phys. Res.*, **2024**, 6, 73–82.
43. S. Vivekanandan, J.R. Brender, S.Y. Lee, A. Ramamoorthy, A partially folded structure of amyloid-beta (1–40) in an aqueous environment, *Biochem. Biophys. Res. Commun.*, **2011**, 411, 312–316.
44. A. Santoro, M. Buonocore, M. Grimaldi, et al., Monitoring the conformational changes of the A $\beta$  (25–35) peptide in SDS micelles: a matter of time, *Int. J. Mol. Sci.*, **2023**, 24, 971.
45. J. McLaurin, T. Franklin, X. Zhang, J. Deng, P.E. Fraser, Interactions of Alzheimer amyloid-beta peptides with glycosaminoglycans: effects on fibril nucleation and growth, *Eur. J. Biochem.*, **1999**, 266, 1101–1110.